Task XIX

DETERMINING MORPHOLOGY OF LANGMUIR MONOLAYERS AT THE LIQUID-GAS INTERFACE

I. Aim of the experiment

The aim of the classes is to determine the morphology of Langmuir monolayers formed by selected membrane lipids at the water-air interface using the Brewster angle microscope.

II. Introduction

1. Membrane lipids - structure and classification.
2. Methods of model biological membranes preparation.
3. Langmuir monolayers.
4. Determination of surface tension and pressure using the Wilhelmy plate method.
5. Determination of π-A isotherms.
6. Refractive index and Brewster angle.
7. Principle of the Brewster angle microscope operation.
8. Applications of Brewster angle microscopy.

Bibliography:

1. Lecture, *Model biological membranes. Preparation, characteristics and applications.*
2. A. Chyla, *Warstwy Langmuira-Blodgett i ich zastosowanie w elektronice molekularnej*, Oficyna Wydawnicza Politechniki Wrocławskiej, Wrocław, 2004.
3. M. Bryszewska, W. Leyko, *Biofizyka dla biologów*, PWN Warszawa, 1997.
4. E. T. Dutkiewicz, *Fizykochemia powierzchni*, WNT Warszawa, 1998.
5. Task XVII, chapter III.1. http://www.katedrachf.umcs.lublin.pl
6. Task XVIII, http://www.katedrachf.umcs.lublin.pl
7. KSV NIMA LB Software Manual v1.6
8. https://accurion.com/thin-film-characterization/products/nanofilm-ultrabam

III. Theory

III. 1. Brewster Angle Microscopy - Introduction

The phenomenon of light reflection from various surfaces is part of our everyday life. However, one of the surprising optical properties is the ability to obtain the conditions where no reflection is observed. This is the case for a perfectly clean interface, at which *p*-polarized radiation is incident at the angle, called **Brewster angle.** Any change in the optical properties in the interfacial region will lead to the reflection of the incident radiation. This fact is the basis of *Brewster Angle Microscopy* (**BAM**), a modern technique for studying nanofilms at the water-air interface and on the surface of transparent dielectric carriers.

The presence of a monolayer of the compound at the interface causes that Brewster's law is not fulfilled and the covered part of the surface of the subphase reflects light, albeit with a low intensity. By increasing the radiation intensity, the contrast between the coated and uncoated surfaces can be enhanced with the CCD detector, obtaining high-contrast images of the layer morphology.

III. 2. Brewster's law

Light is an electromagnetic wave, the source of which can be the Sun - a natural source as well as artificial sources (lamp, laser). During the propagation of light, the electric and magnetic field vectors are perpendicular to each other and to the direction of wave propagation (Fig.1).
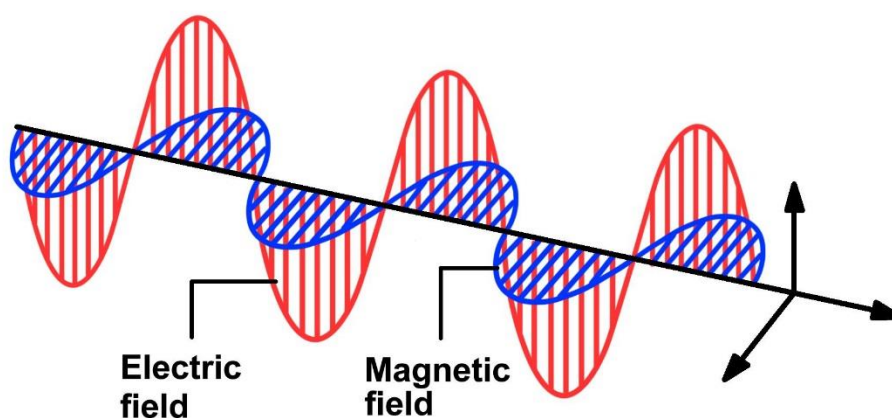

Fig.1. Electromagnetic wave propagation diagram
[https://www.quotemaster.org/electromagnetic+wave].

Light falling on a flat dielectric surface (water, glass) is reflected and partially polarized (Fig. 2). In the case of p-polarized light, the electric field vectors are parallel to the plane of incidence of the light rays and in the case of light with *s*-polarization, the electric field vectors are perpendicular to the plane of incidence of the light rays.
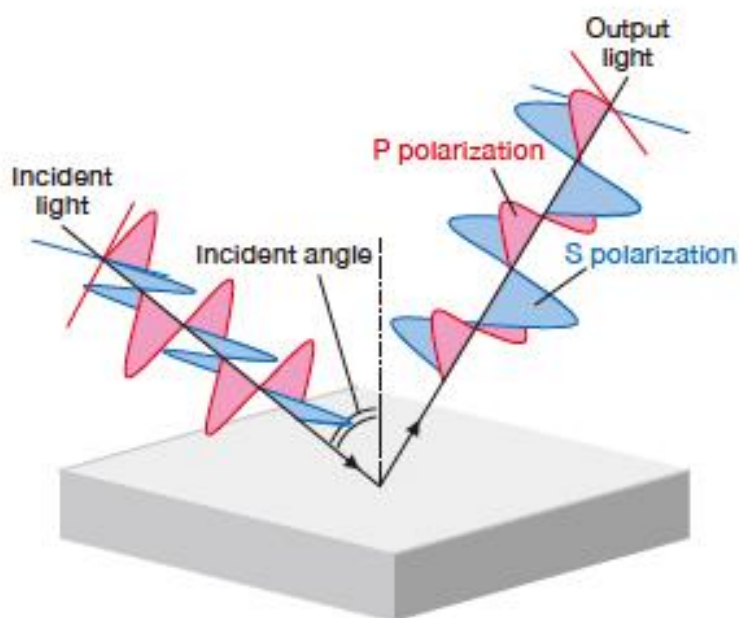

Fig. 2. Polarization of light due to the reflection from the flat dielectric surface [www.global-optosigma.com].

It is believed that the first phenomenon of polarization was discovered and described in the 19th century by the Scottish physicist, mathematician and astronomer Sir **David Brewster.** Owing to his experiments, he noticed that the unpolarized light that hits the surface at an angle, the so-called **Brewster angle**, being reflected, becomes polarized and the angle between the reflected and refracted radiation is 90° (Fig. 3). This property of light reflecting off the surface of dielectrics gave rise to a non-invasive imaging technique called after the creator of this theory, **Brewster angle microscopy**.

In Figure 3 the Brewster angle between the ray of light falling on the surface and the normal (a line perpendicular to the surface from which the light ray is reflected) as well as the angle between the reflected and refracted radiation, which is $90°$, are marked. Typically, the direction of the electric field vector affects the angle at which the light is polarized. The figure shows that the vectors of the electric field of the reflected rays are parallel to the plane from which they are reflected and perpendicular to the plane of incidence of unpolarized radiation, *s*-polarization. The phenomenon of p-polarization occurs when the vectors of the electric field of the reflected light vibrate in the plane perpendicular to the surface from which they were

3

reflected. In Figure 3, the Brewster angle between the ray of light falling on the surface and the normal (a line perpendicular to the surface from which the light ray is reflected) as well as the angle between the reflected and refracted radiation, which is 90˚, are marked. Typically, the direction of the electric field vector affects the angle at which the light is polarized. The figure shows that the vectors of the electric field of the reflected rays are parallel to the plane from which they are reflected and perpendicular to the plane of incidence of unpolarized radiation s-polarization. The phenomenon of p-polarization occurs when the vectors of the electric field of the reflected light vibrate in the plane perpendicular to the surface from which they were reflected (Fig. 2).
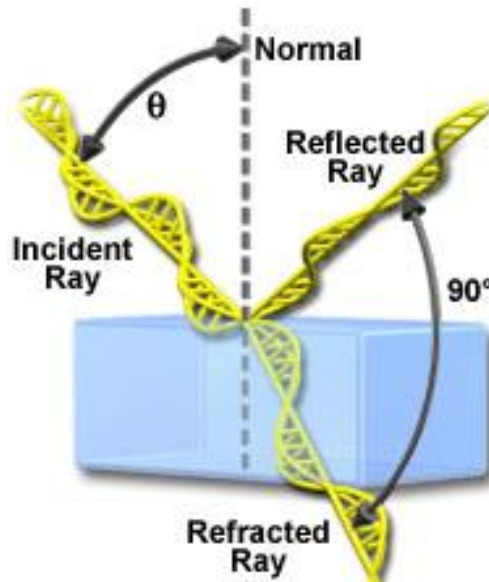

Fig. 3. Scheme of polarization of light reflected from the dielectric surface
[https://micro.magnet.fsu.edu/primer/java/scienceopticsu/polarizedlight/brewster/index.html].

When a beam of light passes trough the boundary between two media with different refractive indices some of the radiation is reflected. Figure 4 shows the dependence of the value of the reflection coefficient $- R$, of light with the p- and s-polarizations on the angle of light incidence $- \theta_i$, at the Fresnel boundary between air and water. The Fresnel limit occurs between two dielectrics, e.g. air and water, which have different refractive indices $- n$, respectively $n_1 = 1$ and $n_2 = 1.33$ changing rapidly in the range from n_1 to n_2.

The reflection coefficient of p- and s-polarized light is calculated according to the Fresnel equations (1) and (2):

$$R_p = \left(\frac{\tan(\theta_i - \theta_r)}{\tan(\theta_i + \theta_r)}\right)^2 \tag{1}$$

$$R_s = \left(\frac{\sin(\theta_i - \theta_r)}{\sin(\theta_i + \theta_r)}\right)^2 \tag{2}$$

and Snell (3):

$$n_1 sin\theta_i = n_2 sin\theta_r \qquad\qquad (3)$$

where: θ_i – the angle of light rays incidence,

θ_r – the angle of light rays refraction,

n_1 – the refractive index of the 1st medium (usually air, $n_1 = 1$),

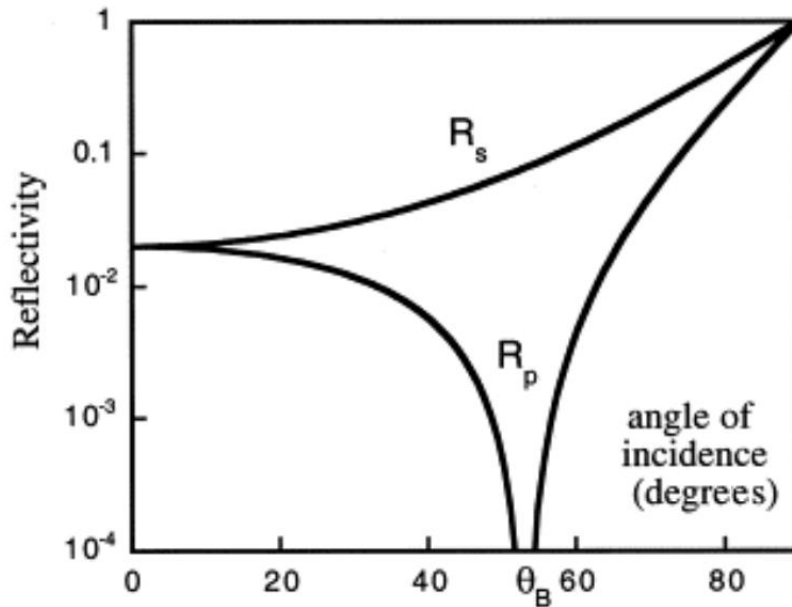n_2 – the refractive index of the 2nd medium (e.g. water, $n_2 = 1.33$).

Fig. 4. Reflection coefficient (R) from the sharp interface as a function of the incidence angle for light with the p-polarization (in the plane of incidence) and s-polarization (perpendicular to the plane of incidence) [*Colloid Surf. A* 171, 2000, 33-40].

Figure 4 shows that in the case of light with polarization s, with increasing the value of the incidence angle – θ_B, the value of R_S increases to that of 1. However the p-polarized light behaves differently because increasing initially the incidence angle of the light rays is accompanied by a decrease in the value of R_p to 0. Further increasing the incidence angle of the rays causes the increase of R_p to the value of 1. The incidence angle for which the phenomenon of reflection of p-polarized light rays is not observed is the **Brewster angle**. This takes place when the beam of the reflected rays is perpendicular to that of the rays refracted at the boundary of two dielectric media (air/water).

Theoretically, when p-polarized light is incident at the Brewster angle at the Fresnel interface between the tested dielectrics, the phenomenon of light rays reflection is not observed, so the radiation reflected from the sharp (so-called *Fresnel*) interface is completely extinguished (Fig. 4). This situation refers to a perfectly sharp, roughness-free boundary between the two transparent media, between which the refractive index changes abruptly. However, in reality the phenomenon of reflection does not disappear, but is observed to a minimal extent, i.e. the intensity of the reflected radiation is not completely extinguished but reaches a minimum

(1.2·10⁻⁸). The disappearance or limitation of the occurrence of this phenomenon depends on the properties of the interfacial zone, namely on the thickness and unevenness of the boundary (caused by thermal fluctuations) and the anisotropy of the monolayer.

By making the appropriate transformations of the formulae given above and using the relationship:

$$\theta_i + \theta_r = 90^o \tag{4}$$

Brewster angle ($\theta_i = \theta_B$) can be determined knowing the refractive indices of the media on which the beam of light rays falls according to equations (5) and (6):

$$tan\theta_B = \frac{n_2}{n_1} \tag{5}$$

$$\theta_B = arc\ tan\frac{n_2}{n_1} \tag{6}$$

Brewster angle takes a different value at the boundaries between different media. This is due to the different values of the refractive index n in these media. Therefore, the values of the reflection coefficient R are distributed differently, depending on the incidence angle of light θ_i, which is given in the graphs showing this relationship at the air-water and air-glass interfaces (Fig. 5).
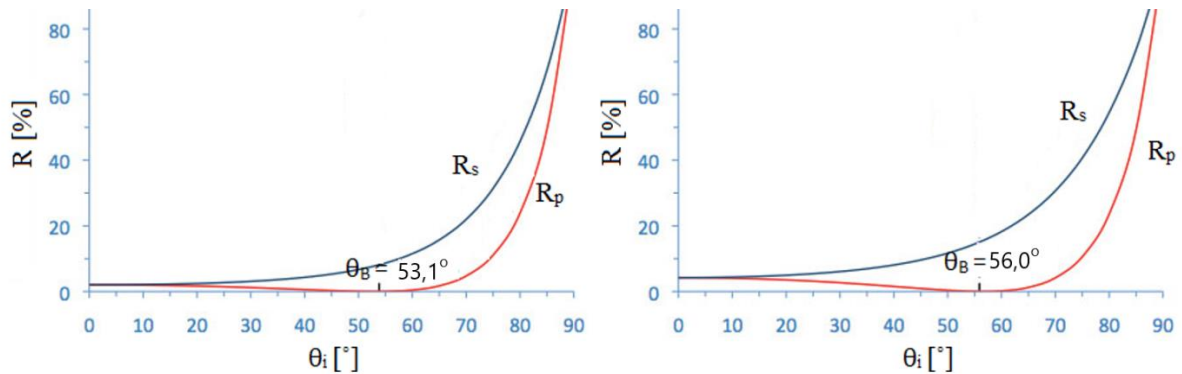
Fig. 5. Value of Brewster angle for the Fresnel boundaries between different media: air-water (left) and air-glass (right) [www.cameratechnica.com].

III. 3. Principle of the Brewster angle microscope operation

The basis of BAM microscopy is the use of the Brewster angle and the properties of *p*-polarized light incident on the boundary between two media at this angle. Because then the phenomenon of light rays reflection is not observed, or is limited, a darkened field is obtained as an image. When a film consisting of one layer of molecules is placed at the interface, the refractive index changes and some of the incident rays are reflected (Fig. 6).

The formation of a monolayer of an amphiphilic substance on the water surface causes a slight change in the value of the Brewster angle due to the appearance of an additional thin

layer with the refractive index different from that of air and water, which leads to an increase in the reflected radiation intensity. For example, the presence of a monolayer at the water-air interface with the thickness of 10 Å and the refractive index of 1.4 contributes to the approximately 35-fold increase in reflectance. Therefore the intensity of the reflected radiation is largely dependent on the properties of the interface.
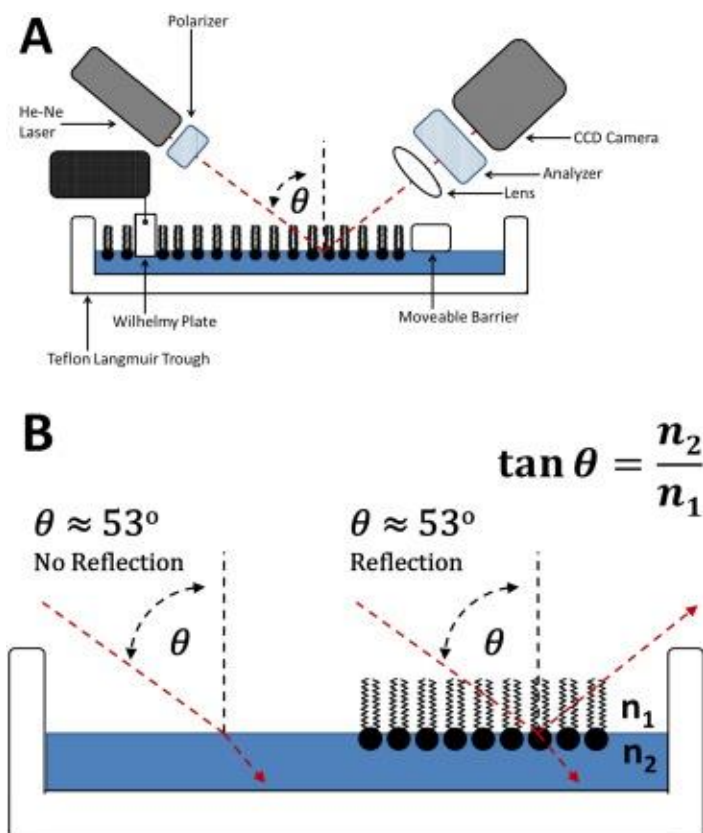

Fig. 6. Scheme of the principle of the Brewster angle microscope operation.

Figure 7 shows the schematic principle of the BAM microscope operation together detailing the basic optical elements of the instrument. A typical BAM kit consists of a light source, polarizer, objective, analyzer and detector. A helium-neon or argon laser can be used as the light source. In most BAM microscopes, the source of light radiation is a laser with the wavelength of 532 nm. A typical detector is the CCD camera, which is a photosensitive silicon wafer.
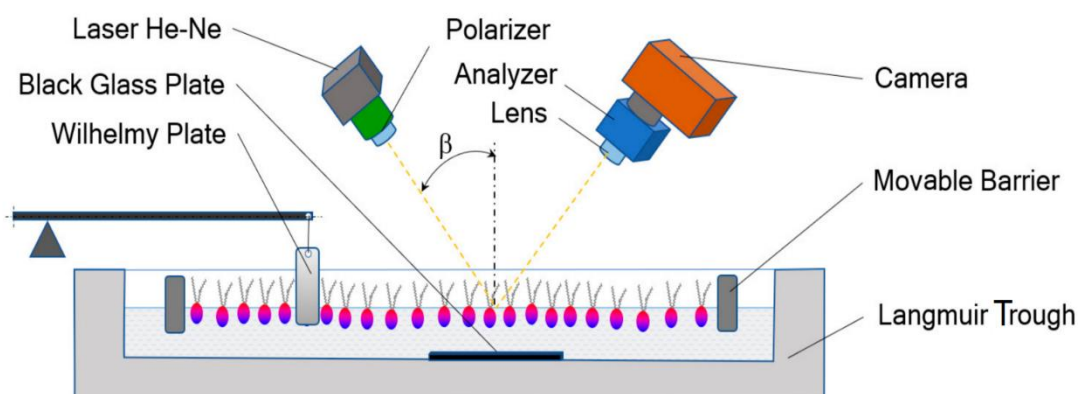
Fig. 7. Diagram showing the basic elements of the construction of the microscope and its principle actions [*Int. J. Mol. Sci.* 22, 2021, 4729].

In order to obtain an image of the monolayer, it is illuminated with high intensity at Brewster angle (which for the water-air interface is 53°) using the *p*-polarized laser beam. The radiation reflected from the surface film is directed trough the lens to the sensitive camera, from which the image is transferred to the computer and the monitor screen. Using modern BAM microscopes, it is possible to observe a fragment of a monolayer with the dimensions of approx. 0.5x0.5 mm^2 with a high resolution of 2 μm in real time. The observed image shows the areas of different brightness, which is the result of the presence of individual molecules and the degree of their packing in the analyzed film. The first images of the Langmuir monolayers taken with the BAM microscope are shown in Figure 8.
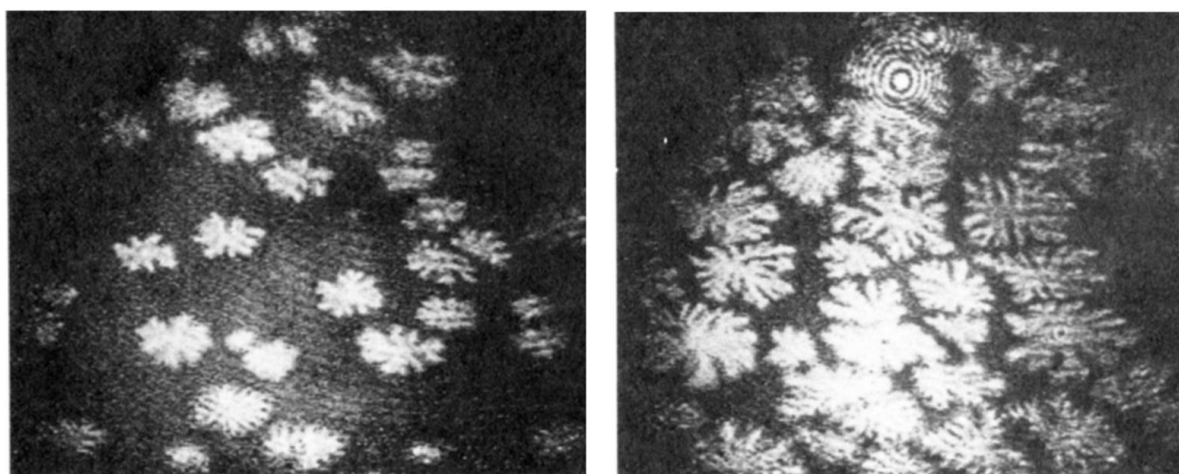
Fig. 8. First images of the Langmuir phospholipid monolayers by Hönig and Möbius in 1991 [*J. Phys. Chem.* 95, 1991, 4590].

III. 4. Application of the Brewster angle microscopy

BAM microscopy is an excellent tool for observing:

–   a physical state of two-dimensional monolayers (Fig. 9)
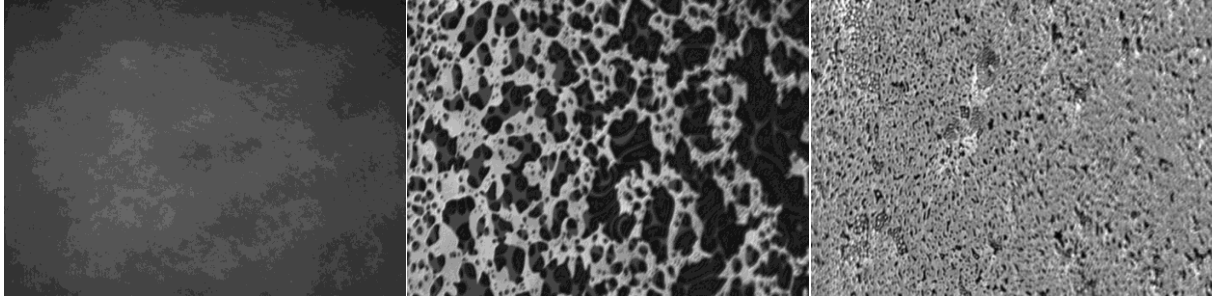
gas → liquid-expanded / liquid-condensed → solid phase

Fig. 9. Monolayers of 1,2-diplamitoyl-*sn*-glycero-3-phosphoglycerol (DPPG).

–   the degree of order and packing of the film in the individual stages of compression at different surface pressures (Fig. 10)
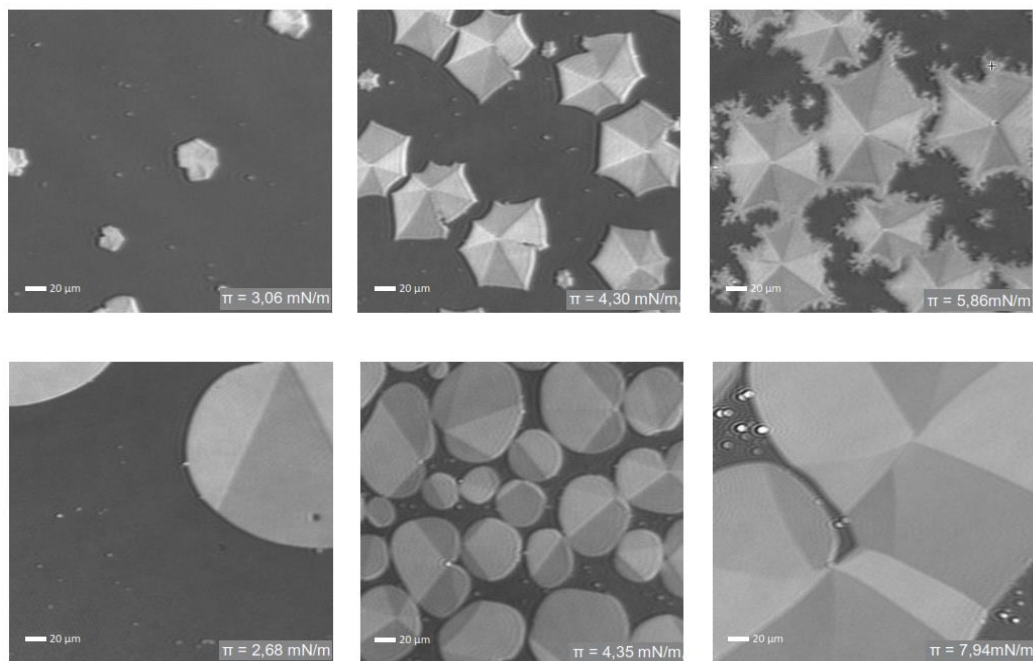

Fig. 10. Monolayers of 2-monopalmitoyl-*rac*-glycerol (top) and 1-monopalmitoyl-*rac*-glycerol (bottom) at different surface pressures [www.accurion.com].

– morphological features of monolayers during compression/decompression, e.g. formation and growth of domains (Fig. 11)

The studies of monolayers morphology lead to a more profound understanding of the two-dimensional structure of their condensed phase. The big advantage is the possibility of direct observation in real time, without the addition of dyes and the need to transfer the films to a permanent medium. In many papers, BAM images are collated directly with the $\pi - A$ isotherm (Fig. 11). For this type of research, it is necessary to integrate the software of the microscope and the Langmuir trough.
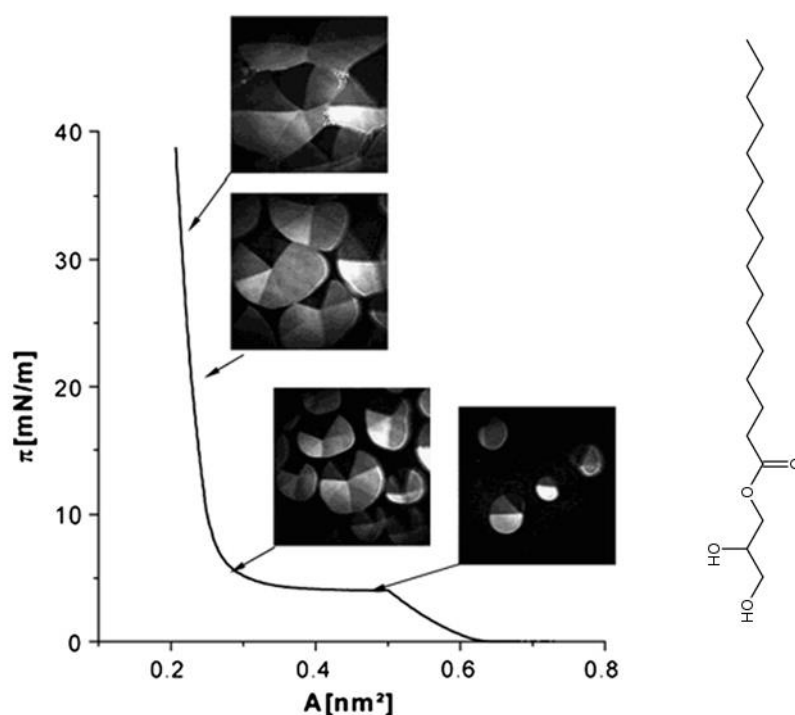
Fig. 11. Domain growth as the 1-monopalmitoyl-*rac*-glycerol monolayer is compressed at 23ºC [*Curr. Opinion Colloid Interface Sci.* 19, 2014, 183-197].

– internal structure of the two-dimensional condensed phase domains (Fig. 12)

Brewster angle microscopy is an effective method to visualize the optical anisotropy of monolayers induced by areas with different orientations of the alkyl chains. The example is the monomolecular film of ethyl stearate presented in Figure 12.
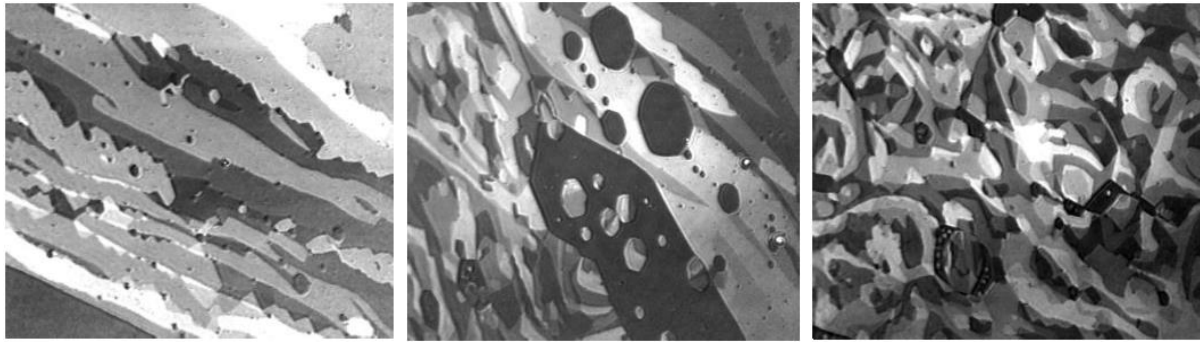
Fig. 12. Ethyl stearate monolayer at π <1 mN/m. Field of view 600 µm² [www.accurion.com].

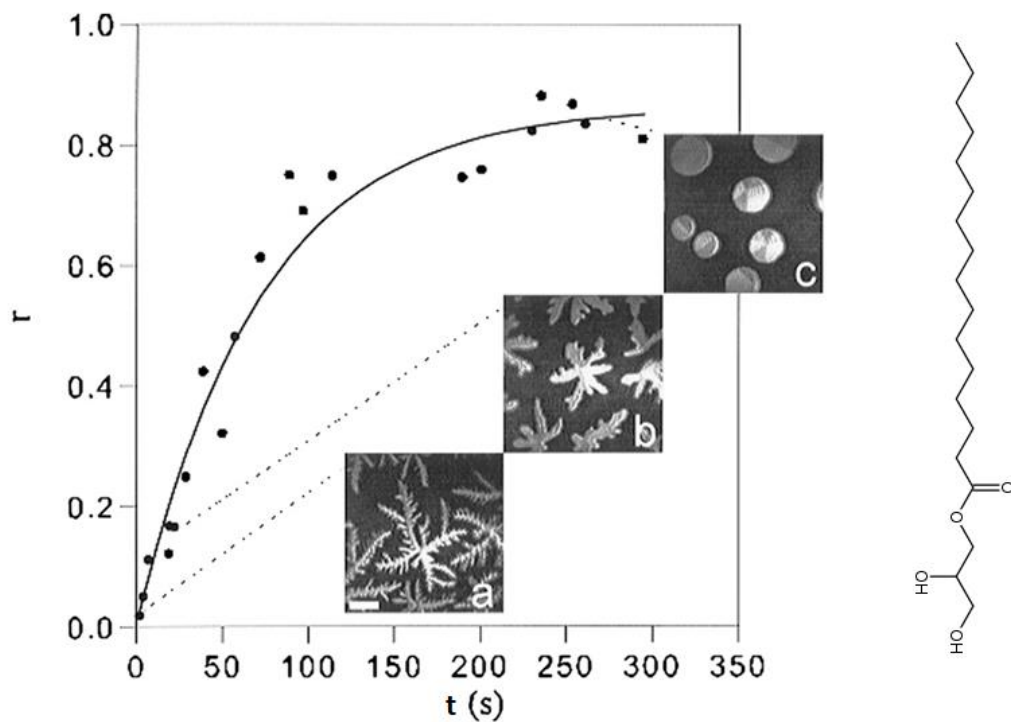   –   <u>changes in the shape of domains over time (Fig. 13)</u>

Fig. 13. Diagram showing the change of sphericity of domains (r) as a function of time (t) in the monolayers of 1-monopalmitoyl-*rac*-glycerol. When the monolayer compression stops in the *plateau* region on the $\pi - A$ isotherm (A = 0.38 nm²/molecule, T=23°C) three types of relaxation domains are present [*Curr. Opinion Colloid Interface Sci.* 19, 2014, 183-197].

  − <u>chiral differentiation of the condensed phase domains (Figs. 14 and 15)</u>

The monolayers of the amphiphilic molecules enantiomers differ. Depending on the type of enantiomer, left-handed or right-handed domains are distinguished.
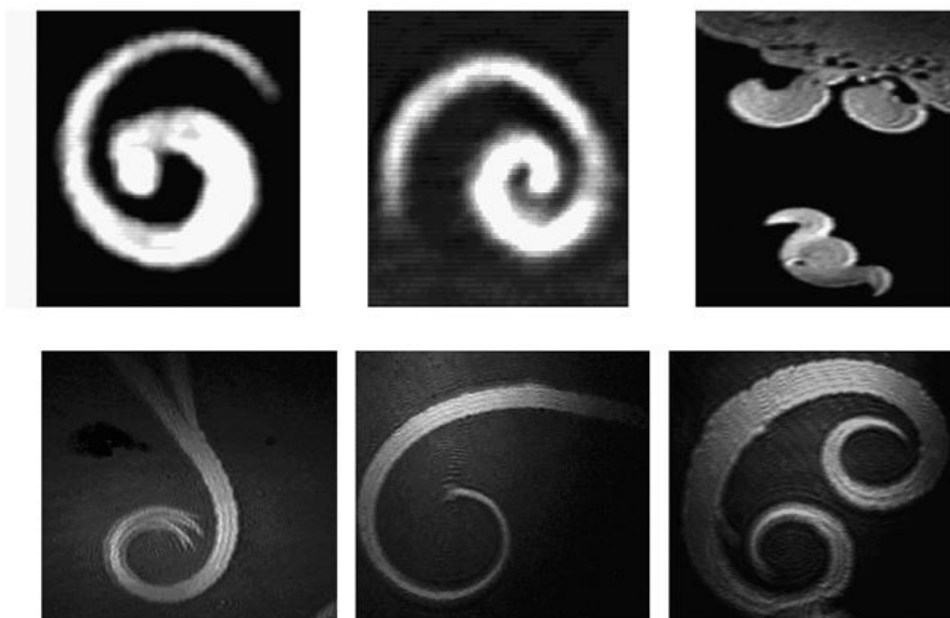
Fig. 14. Chiral differentiation of condensed phase domains of N-stearoylserine methyl ester (top, image size 60x60 µm) and N-α-palmitoylthreonin (bottom, 300x300 µm), (left) D-enantiomer; (middle) L-enantiomer; (right) 1: 1 DL-racemate [*Phys. Chem. Chem. Phys.* 13, 2011, 4812-4829].
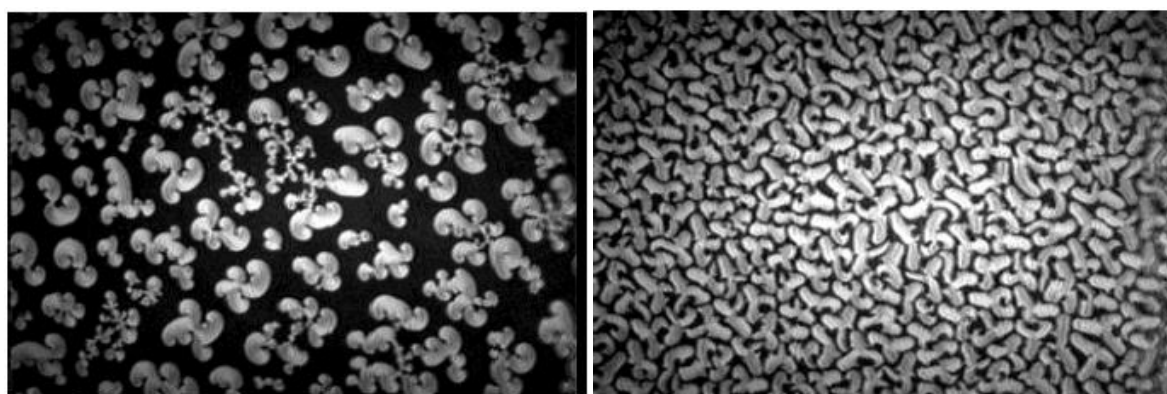
Fig. 15. Chiral differentiation of D-dipalmitoyl-*sn*-glycero-3-phosphocholine (D-DPPC) and racemate (DL-DPPC) condensed phase domains [www.accurion.com].

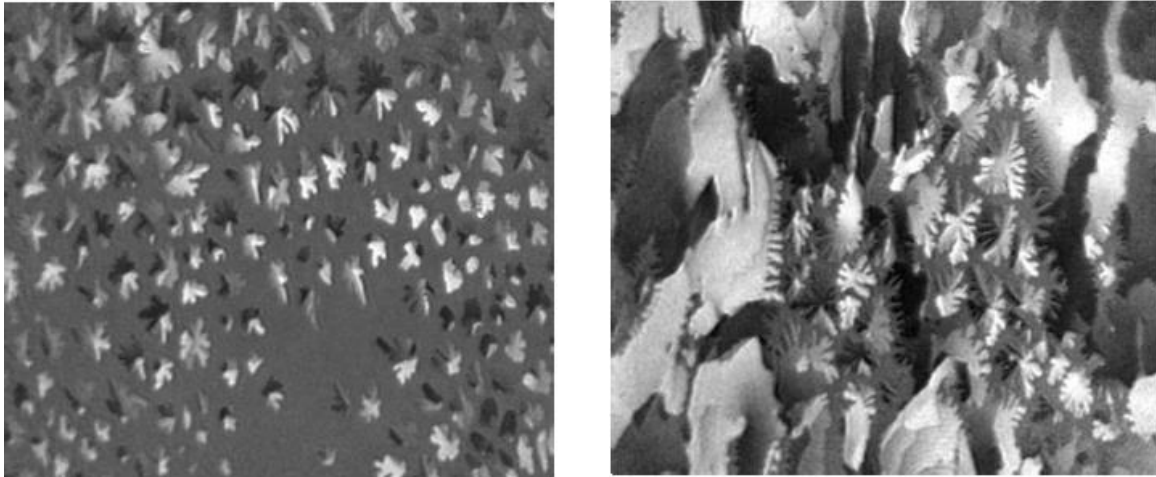– phase transitions, detection of phase transitions (Fig. 16)

Fig. 16. Monolayer of 1,2-dimyristoyl-*sn*-glycero-3-phosphoethanolamine (DMPE) during the first order phase transition (LE-LC) [www.accurion.com].

– transformation of monolayers into the multilayer structures (Fig. 17)
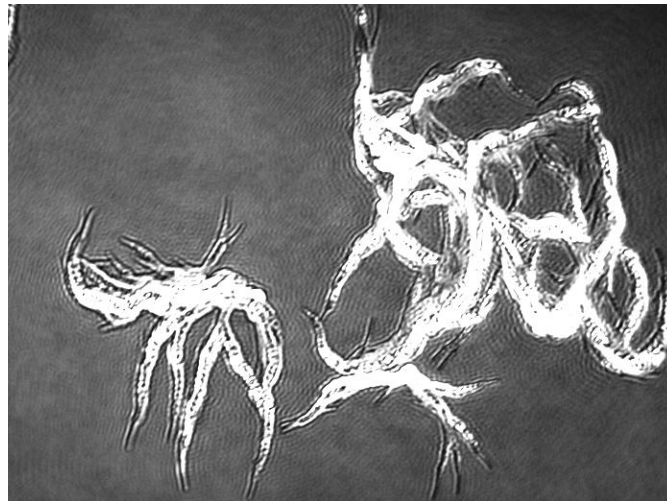

Fig. 17. Lauryl gallate (LG) monolayer after the collapse [www.accurion.com].

– influence of ions/substances, including surfactants, contained in the aqueous phase on the properties of surface films (Fig. 18)
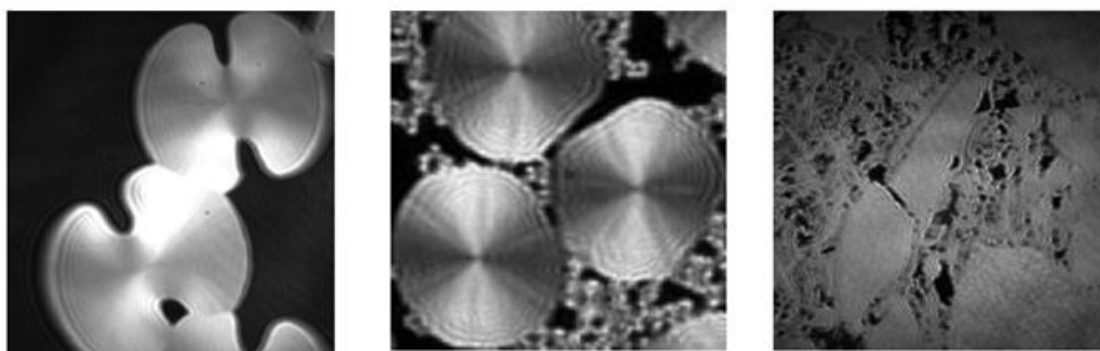
Fig. 18. Supramolecular domain structures of melamine on different subphases: the aqueous solutions of thymine (left), uracil (middle) and barbituric acid (right) [*Phys. Chem. Chem. Phys.* 13, 2011, 4812-4829].

– phase separation or partial miscibility in the monolayers and thin films (Fig. 19)
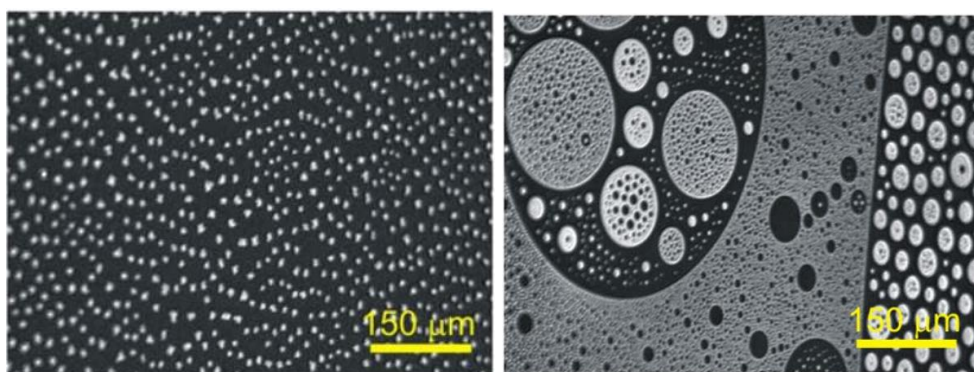

Fig. 19. Partial miscibility in the DPPC-DOPC monolayer (left) and DPPC-DOPC-Chol (right), where: DPPC – 1,2-dipalmitoyl-*sn*-glycero-3-phosphocholine, DOPC – 1,2-dioleoyl-*sn*-glycero-3-phosphocholine, Chol – cholesterol [*J. Membrane Biol.* 251, 2018, 277-294].

– surface structures in the adsorption films
– monolayers formed by: fullerenes, crown ethers, polymers or organometallic compounds without amphiphilic properties

- microscopic observation of changes in the structure of monolayers as a function of temperature (Fig. 20) allows to create phase diagrams of amphiphilic substances
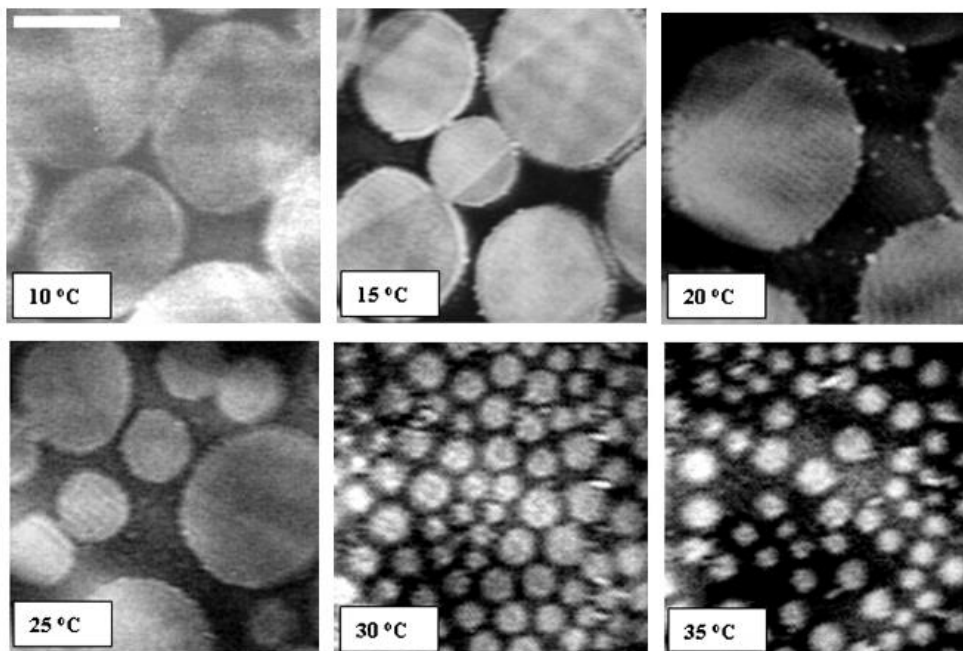

Fig. 20. Influence of temperature on the behaviour of 2-hydroxyethyl myristate monolayers. 100 µm scale [*Appl. Surf. Sci.* 257, 2010, 1129-1133].

- in combination with other techniques, it can also be used to estimate the inclination angles of molecules in individual phases of the monolayer (Fig. 21)
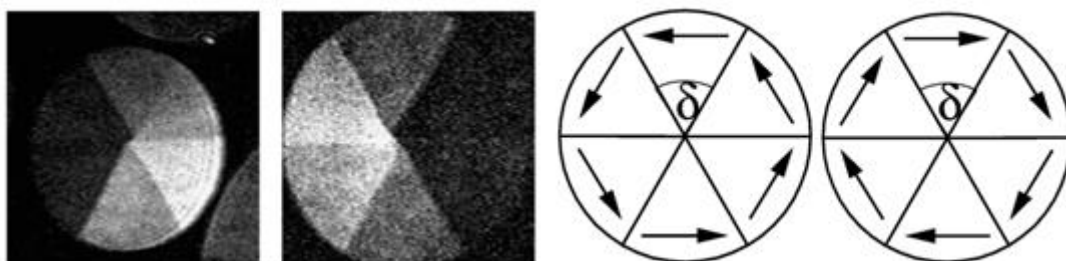

Fig. 21. Ethyl palmitate domains divided into 6 segments. Below is a diagram of the direction of inclination of the alkyl chains perpendicular to the bisectors of the domains [*Curr. Opinion Colloid Interface Sci.* 19, 2014, 183-197].

- gives the ability to measure the thickness of monolayers as well as to observe the separation of microphases and the behavior of mono- and multilayers during their disintegration

IV. Experimental

A. Apparatus and materials

1. Apparatus:
- Langmuir-Blodgett KSV 2000 Standard trough with the area of 780 cm^2, equipped with two barriers and a platinum Wilhelmy plate (circumference 39.24 mm) for surface pressure measurements, coupled with a computer,
- antivibration table,
- thermostat, Lauda
- water pump, Air Liquide,
- Bunsen gas burner, Labrant,
- dark glass bottles with caps with the capacity of 5 cm^3 – 3 pcs.,
- beakers with the capacity of 50 cm^3 – 3 pcs.,
- automatic pipette with the 1 cm^3 tip – 1 piece,
- microsyringe with the capacity of 100 μL – 1 item, Hamilton,
- tweezers – 1 pc.,
- spoon-spatula – 3 pcs.

2. Reagents:
- 1,2-dipalmitoyl-*sn*-glycero-3-phosphocholine (DPPC), ≥ 99%,
- 1,2-dioleoyl-*sn*-glycero-3-phosphocholine (DOPC), ≥ 99%,
- cholesterol (Chol), ≥ 99%,
- acetone, pure p.a.,
- methanol, pure p.a.,
- chloroform, pure p.a.,
- deionized and demineralized water from the Milli-Q system with the resistance of 18.2 MΩcm and pH 5.6.

3. Accessories:
- dust-free wipes,
- powder-free nitrile gloves,
- filter paper,
- parafilm.

B. Task scheme

1. Preparation of lipid solutions in chloroform.
2. Preparation of Langmuir trough and Brewster angle microscope for measurements.
3. Creation of Langmuir monolayers of the tested lipids.
4. Observation of monolayer morphology with the simultaneous determination of $\pi - A$ isotherms during the symmetrical compression process.
5. Taking pictures at different values of surface pressure.

C. Apparatus and software service

The Brewster angle microscope, UltraBAM by ACCURION (Figs. 22 and 23), is an instrument coupled to the Langmuir-Blodgett (LB) KSV NIMA trough and a computer controlled by the Nanofilm-UltraBAM software. Operation of the LB trough and the KSV NIMA LB software is discussed in the script for Task **XVIII.**
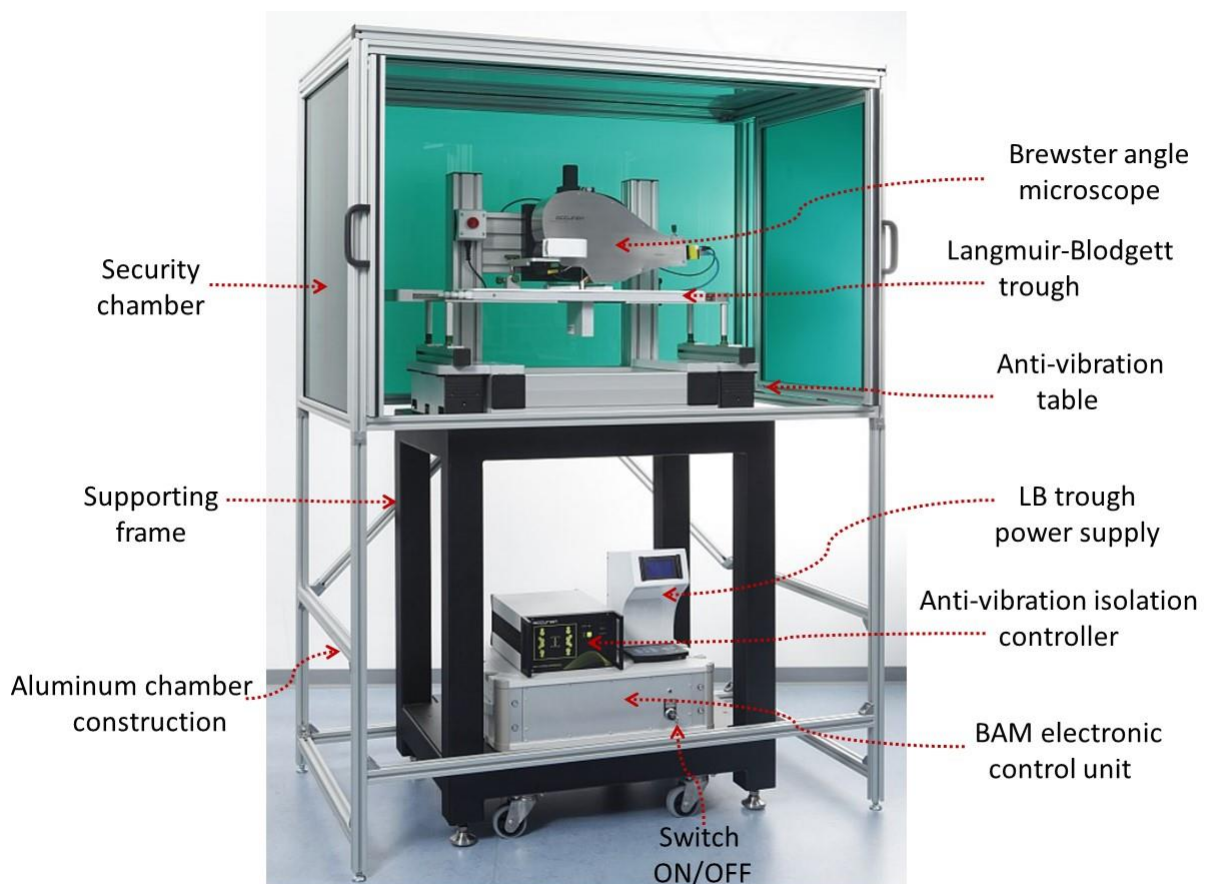

Fig. 22. Set: Brewster angle microscope Nanofilm-UltraBAM coupled with the Langmuir-Blodgett KSV NIMA trough, in the chamber protecting against harmful laser radiation, stable table + anti-vibration isolation controller, LB trough power supply, BAM electronic control unit.

The chamber has a protective function against dust and air movements as well as against scattered laser light. The wavelength of the laser radiation is in the red colour range (658 nm), and the green colour of the walls is a complementary colour.
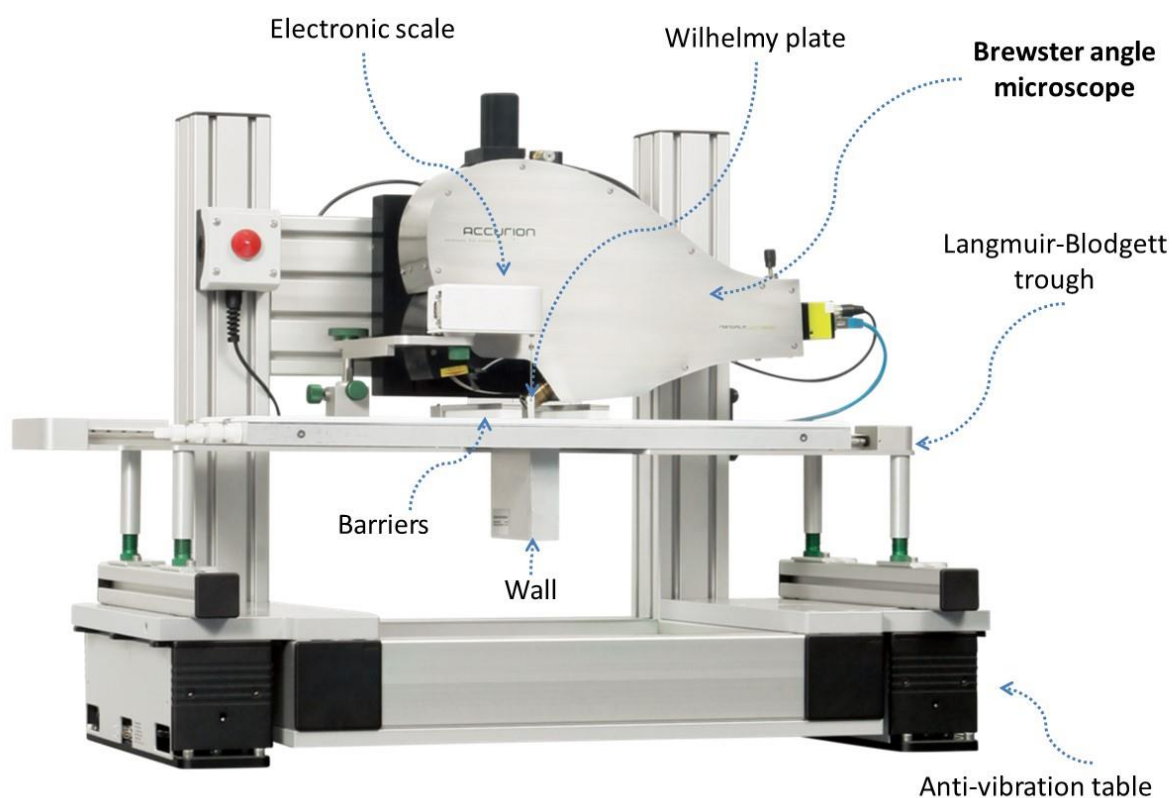
Fig. 23. Brewster angle microscope Nanofilm-UltraBAM coupled with the Langmuir-Blodgett KSV NIMA trough.

Below are the specific steps you need to take:

– switch the computer,
– turn on the thermostat by setting the desired temperature,
– turn on the anti-vibration isolation controller,
– switch on the power supply unit and trough software LB,
– prepare the trough for measurements according to the instructions given in Task **XVIII**,
– switch on the BAM electronic control unit by turning the switch (key) to the ON position,
– run the Nanofilm-UltraBAM software by clicking three icons in turn, the following windows will open simultaneously (Fig. 24):
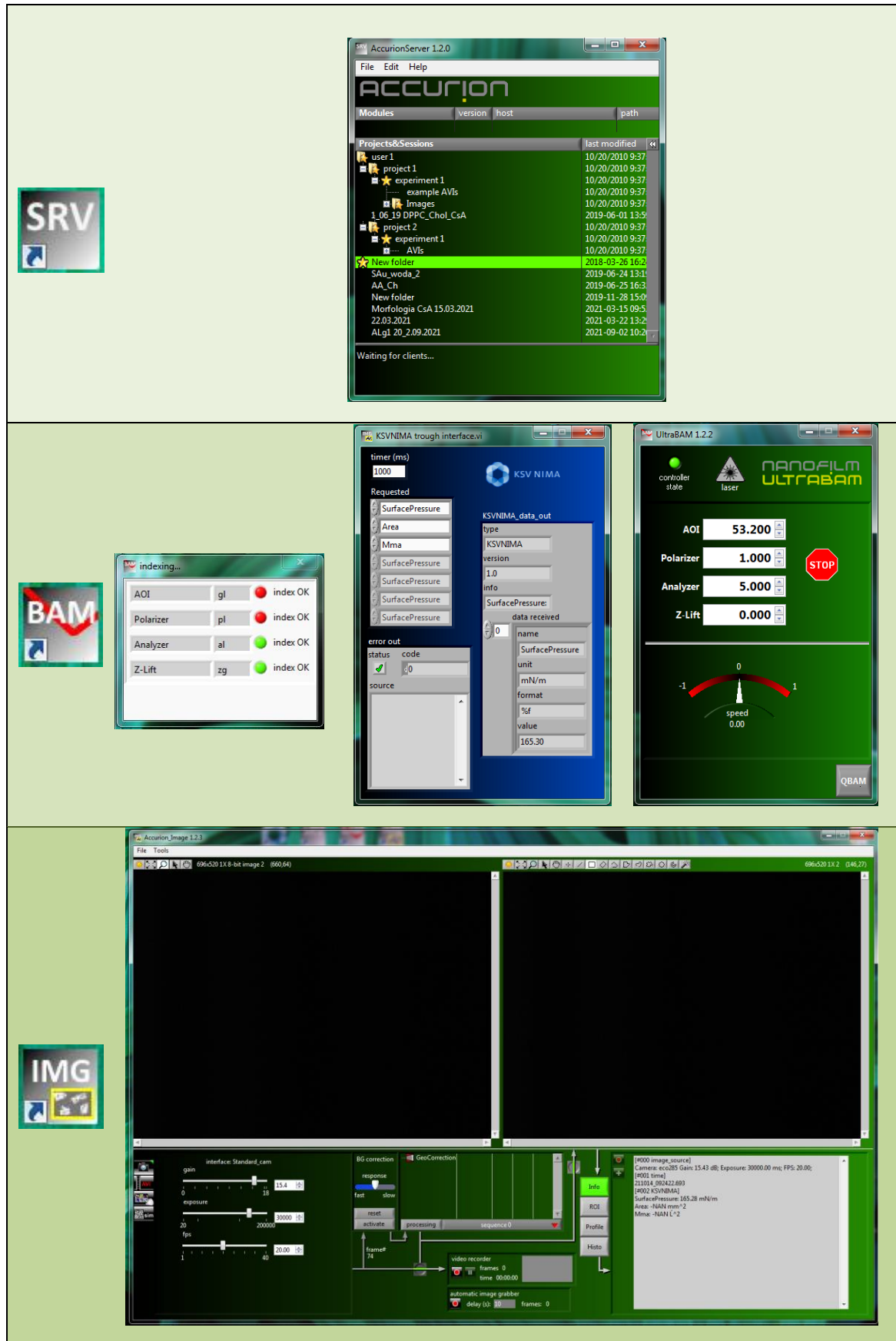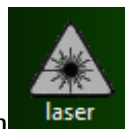
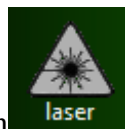**Fig. 24.** Nanofilm-UltraBAM software icons and windows.

Icon ![SRV] launches the Accurion Server window. It is used to collect data, which is saved by default in the active (marked in green) folder.
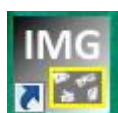
Icon ![BAM] launches the UltraBAM window which is used to control the operation of individual elements of the microscope:

- laser can be initiated by clicking on the icon ![laser] which is highlighted ![laser] the activation stage takes a few seconds,
- selection of the angle of incidence (Brewster, AOI), polarizer, analyzer and head height (*Z-lift*) from the liquid surface. Values must be entered manually or set using the *Speed control*. In the second case, place the mouse cursor on the value and drag it to the left or right.
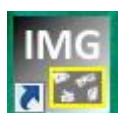
Icon ![IMG] launches the Accurion Image window, which allows to observe the monolayer at the liquid-gas interface and takes pictures of the surface. Before the measurement, the image exposure and gain parameters as well as the number of frames per second should be adjusted in relation to the cleaned surface of the subphase.
→→→

Images are made by clicking ![sun icon]

You can view them using the option ![view icon]

and return to the shooting mode. ![camera icon]

Pictures can be taken with or without the background correction.

In the first case, activate the option by clicking the activate button.
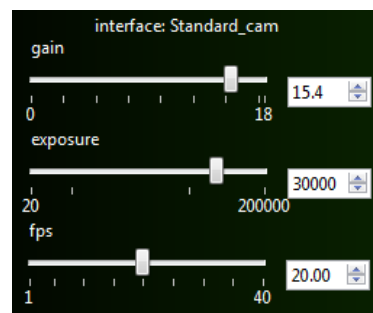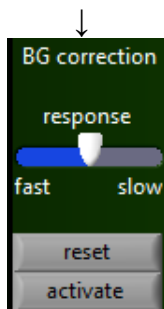
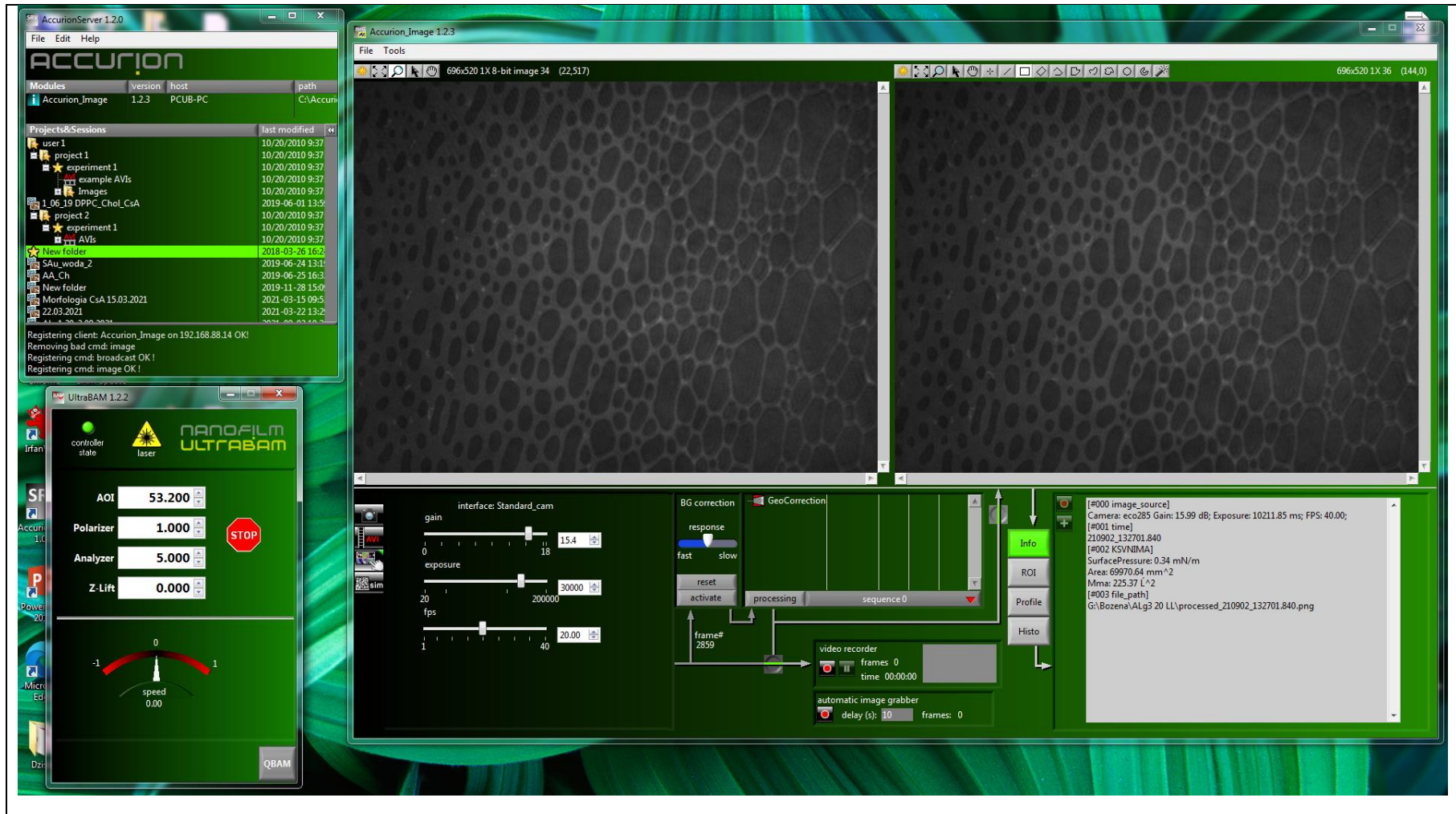The preview of the monitor after the comprehensive software launch is given in Fig. 25.

Fig. 25. Preview of the monitor screen after the comprehensive launch of the Nanofilm-UltraBAM software.

D. Program of activity

Preparation of solutions. Make solutions of lipids in chloroform. For this purpose, in 5 cm^3 bottles made of dark glass, weigh about 1 mg of a given lipid using an analytical balance (Sartorius), and then dissolve the sample in such an amount of chloroform to obtain a solution with a concentration of 1 mg/mL. Prepare all lipid solutions in the same way. Close the bottles with the solutions tightly with the caps and protect against evaporation of the solvent by wrapping them with parafilm, and then store under the cover in the chloroform atmosphere.

Preparation of the LB trough for measurements. Activate the thermostat connected to the Langmuir trough, setting the temperature to 20°C. Before the measurements, clean the Teflon trough and the polyacetal barriers with dust-free wipes soaked in acetone and after the solvent evaporation (approx. 10 minutes) with methanol wipes, using powder-free nitrile gloves and tweezers. After 10 minutes rinse the trough and barriers several times with ultrapure water, which should be removed from the trough using a water pump equipped with a plastic, replaceable tip. Then pour water so that a convex meniscus is formed and clean the subphase surface by sucking out any impurities while the barriers are moving towards the center of the trough. After cleaning the water level should be equal to the trough edges.

Preparation of the BAM microscope for measurements. Start the Brewster angle microscope and the Nanofilm-UltraBAM software as described in point C. Then remove the protective lens cap. Place the black glass plate flat over the trough well, directly under the lens (Fig. 26), so that its slanted (wedge-shaped), smooth part faces the objective lens. The plate arranged in this way absorbs the refracted beam of laser radiation, preventing it from getting into the optical system and minimizes light scattering in favour of imaging quality.
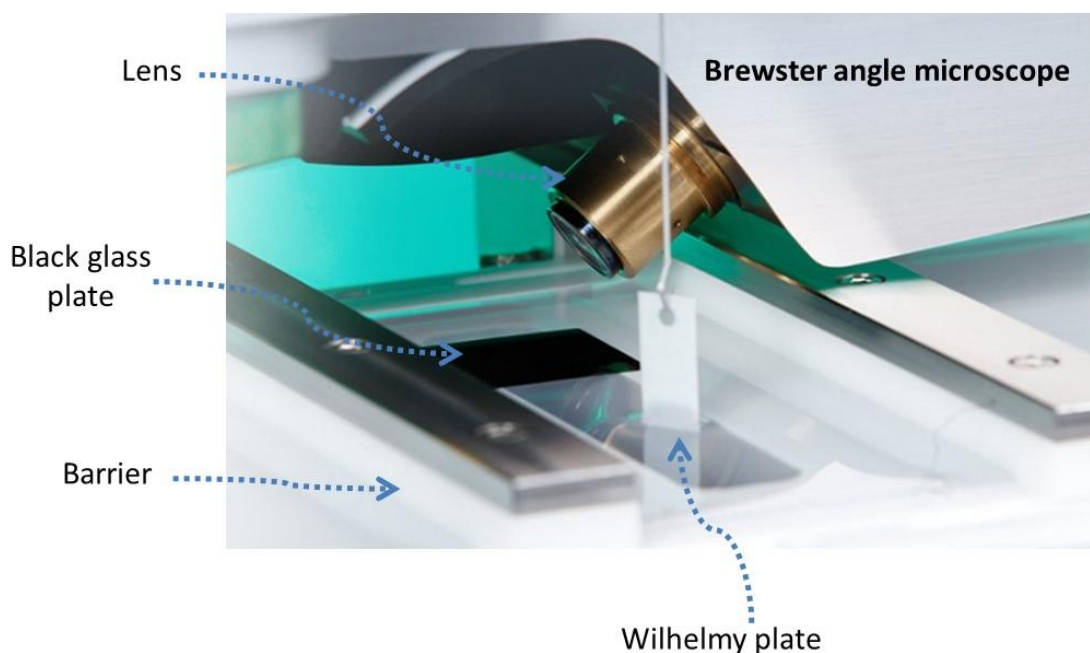

Fig. 26. Method of arranging a black glass plate under the microscope objective.

Examining the surface cleanliness. In order to examine the subphase purity, a platinum Wilhelmy plate with the dimensions of 10x19.62 mm^2 should be rinsed in methanol and water, roasted three times in a burner flame and hung on the balance hook in such a way that 1/3 of the plate is immersed in the subphase. Then, zero the scale and the bars in the Open position, and start compression. The surface pressure is measured by weighing a platinum plate immersed in the subphase. If changes in the surface tension during the movement of the barriers towards the center of the trough do not exceed 0.3 mN/m, the surface of the subphase is considered clean and after opening the barriers, the main measurement starts.

Otherwise, cleaning must be repeated.

Main measurement. Open the lens shutter by turning the knob to the O position. Close the safety chamber door and initialize the laser. Lower the head so that the laser spot is focused on the sloping part of the black plate. Then adjust the parameters of the AOI (53.2º), polarizer, analyzer and camera to obtain a sharp image of the subphase surface (shaded area). Take a picture. Turn off the laser or close the shutter by turning the knob to position C. Then, after zeroing the surface pressure and the position of the barriers, drop the appropriate volume of lipid solution using the Hamilton microsyringe with a Teflon plunger tip. The dosed volume should be selected in the KSV NIMA LB program based on the molar mass of the compound and the concentration of the solution. Typically, the volume is in the range of 50 to 100 µL. After applying the chloroform solution to the water surface, wait 10 minutes for the solvent to evaporate, then turn on the laser and/or open the shutter and start compression at the rate of 10 mm/min. After adjusting the focus, take photos of the monolayer surfaces at various stages of compression (minimum 10 photos). If the morphology changes quickly, take photographs more often. At the same time, the process will be recorded in the form of the dependence of the surface pressure on the surface of the subphase per single molecule in the monolayer ($\pi - A$ isotherms), visible on the computer screen connected to the trough. After completing the measurement, turn off the laser and move the microscope head away from the surface of the subphase. Then remove the contents of the trough and clean it according to the procedure described above. Repeat this for other lipids.

Save the recorded images of the monolayer morphology on the computer along with the values of the corresponding surface pressures. **Failure to save the images may result in their loss when the Accurion Image window is closed!**

Pour the organic solutions remaining after the measurements into the bottle marked **"Chloroform BEAKERS".** Rinse the bottles with screw caps three times with fresh portions of chloroform and allow to dry.

E. Results and discussion

The obtained experimental data should be developed according to the following points:

1. Plot the $\pi - A$ isotherms by plotting the surface area per molecule, A, expressed in Å^2 on the abscissa, and the corresponding surface pressure, π, on the ordinate.
2. Under the graph for a given compound, collate the monolayer morphology images with the information on the surface pressure and surface area per molecule at which they were recorded. Crop images if necessary. Enter the size of the imaging area in μm.
3. Assign the monolayer morphology changes to the specific sections of isotherm (Fig. 11).
4. Compare and describe the morphology images of individual monolayers in terms of film homogeneity, shape and size of domains being formed, phase transitions, chirality, type of multilayer structures after the film collapse.